Phyton-
International Journal of
Experimental Botany

Tech Science Press

DOI: 10.32604/phyton.2021.015533

ARTICLE

Structural and Histochemical Features of the Slow-Growing Perennial *Coptis chinensis* Franch. (Ranunculaceae)

Jingyuan Yang[1], Jie Zhou[1], Jiaojiao Jin[1], Yi Li[2], Xia Zhang[3], Teng Li[3], Mengdi Zhang[3], Xiaodong Cai[3], Chaodong Yang[3] and Cunyu Zhou[3,*]

[1]Hubei Province Key Laboratory of Conservation Biology for Shennongjia Golden Monkey, Shennongjia National Park Administration, Muyu Town, 42400, China

[2]Ningxia Jiesi Environmental Protection Technology Co., Ltd., Yinchuan, 750000, China

[3]Engineering Research Center of Ecology and Agriculture Use of Wetland, Ministry of Education, Hubei Key Laboratory of Waterlogging Disaster and Agricultural Use of Wetland, Yangtze University, Jingzhou, 434025, China

[*]Corresponding Author: Cunyu Zhou. Email: zhoucy@yangtzeu.edu.cn

Received: 26 December 2020 Accepted: 12 March 2021

ABSTRACT

Huanglian (*Coptis chinensis* Franch.) is a slow-growing perennial medicinal herb with considerable economic value. This study aimed to determine the structural characteristics and the levels of berberine deposits in the organs and tissues of Huanglian using light and epifluorescence microscopy. The adventitious roots are composed of primary and secondary structures with endodermis, exodermis, and phellem. The rhizome structures are composed of primary and secondary structures with cuticle and phellem. The leaves are composed of sclerenchymatous rings, isolateral mesophyll, and thin cuticles. We detected berberine in the xylem walls of the roots and rhizomes as well as in the sclerenchymatous rings of the petioles. We postulate that as the exodermis is developed, the deposition of berberine in the xylem closest to the root tips may affect water and nutrient absorption and transfer. Leaf blades had a thin cuticle and isolateral mesophyll, suggesting shade tolerance. These structural and histochemical features suggest that Huanglian is adapted to the slow growing nature of a shady environment.

KEYWORDS

Berberine deposition; *Coptis chinensis*; histochemistry; structure

1 Introduction

Coptis chinensis Franch. (Huanglian) is a perennial medicinal herb in the family Ranunculaceae that is widely cultivated in southwest China. The plant has high economic value due to its berberine content. However, the plant grows slowly, only being suitable for harvesting after about 5–6 years of cultivation [1–5]. Huanglian has isolateral leaves and lacks differentiated tissues in the mesophyll, suggesting that it is intolerant of strong sunlight and is adapted to shady environments, and that it likely also has low photosynthetic efficiency [6–8]. Moreover, the morphologies of sun and shade plants are visibly different [9–10]. The leaves of shade plants are large, with large cells, few mesophyll tissues, and decreased numbers of stomatal [11–14]. Apoplastic barriers, such as the endodermis and exodermis, block absorption of water and minerals in the roots [15–19]. Berberine hemisulfate has been used to test the

permeability of barriers in various plants [16–20]. Structures of adventitious roots and rhizomes of Huanglian have been described using paraffin-sectioning methods [21,22]; the development of endodermis and exodermis in roots has not been detected.

The location of berberine in Huanglian can be determined by the potassium mercuric iodide method. Lu et al. [22] reported that berberine is deposited in the parenchyma tissue of the rhizome sections *in situ*. Brundrett et al. [23] found that the Casparian bands and lignified cell walls fluoresced yellow under UV light when stained with berberine hemisulfate in other species [16,17,24,25]. We speculated that the berberine deposits in the lignified organs might be toxic to the plant or may hinder absorption and transfer of water and nutrients, thereby slowing plant growth [16,18,19,22–25].

In this study, our aim was to investigate whether the anatomical and histochemical features of Huanglian indicate that it is a slow-growing plant adapted to a shady environment. Additionally, we proposed that berberine deposits in tissues of Huanglian could be used to observe autofluorescence of the anatomical structures under UV light and histochemical methods for barriers, thus enabling examination of the structures that characterize the adventitious roots and rhizomes of this shade-tolerant plant. We also sampled the leaves of Huanglian in the sun and shade to identify morphological and anatomical traits that suggest adaptation to shady environments. The leaves exhibited the same traits observed in other species such as *Panax* spp. Evidence of such adaptive characteristics might help explain the ability of Huanglian to grow in shady environments. Our results may also inform future studies of the *ex situ* conservation, taxonomy, evolution, and phylogeny of this shade-tolerant plant and its relatives.

2 Materials and Methods

2.1 Plant Resourcing and Collection

Huanglian samples were collected from 40 plants cultivated under a shading structure in Muyu County of Shennongjia Forestry District, Hubei Province, China on June 02, 2019. We collected intact plants between one and five years of age along with the associated soil. Five plants of each age were collected. All samples were fixed in formalin–acetic acid–alcohol (FAA) for the two-day trip back to the lab. Once there, at least five samples were assessed [26]. A sponge and water were used to remove any excess soil from the samples, which were then immersed in deionized water prior to sectioning. Full-length sections were made of the adventitious roots, rhizomes, and leaves.

The adventitious roots, which are about 75 mm in length each, were sectioned at 10, 20, 30, 40, and 50 mm from the tips. We selected rhizomes and leaves of varying maturity levels (from one to five years old). Young and mature stem sections were made from the visibly elongated internodes. Sections were made from the bases of mature petioles and the centers of the blades (not at the margin).

2.2 Microstructure and Histochemistry

The adventitious roots, rhizomes, and leaves of samples were freehand sectioned under a stereoscope (JNOEC JSZ6, Nanjing, China). Sections were stained with Sudan red 7B (SR7B) for the suberin lamellae [27], with berberine hemisulfate–aniline blue (BAB) for the Casparian bands and lignified walls [23,24], and with phloroglucinol–HCl (Pg) for lignin [26]. Concentrated sulfuric acid digestion was used for the Casparian bands [24,28]. Some sections were not stained exogenously but were examined for berberine autofluorescence under UV light [23,25]. The specimens were examined using bright field microscopy (Leica DME, Weztlar, Germany) and epifluorescence microscopy (Olympus IX71, Tokyo, Japan) and photographed [16,25]. Double-distilled water was used to remove excess stain, and the sections were kept in double-distilled water or appropriate solutions.

2.3 Leaf Blade Data Collection and Statistical Analysis

The lengths and widths of leaves were measured with a centimeter ruler. Tissue thickness data were collected from sections stained with SR7B and BAB as discussed above. We sectioned the leaflet at the center of the blade (not along the margin) to measure the stomata, the number and size of cells, tissue density, and epidermal features. All sections included five blade samples that remained unstained and were mounted with sterile water. Specimens were observed under a Leica DME microscope with a micrometer. Differences in the morphological and anatomical traits between sunny and shady blades were analyzed with paired-samples *t*-tests using SPSS (version 13.0, SPSS Inc., USA) [14].

3 Results

3.1 Berberine Deposits in the Root Tissues

Based on the number of protoxylem poles, the primary xylem in all the root samples was varied from diarch to hexarch (Figs. 1A–1E). At 10 mm from the root tips, the primary xylem autofluoresced yellow, whereas in the cortex and hypodermis or exodermis, the walls fluoresced only faintly (Fig. 1A). At 30 mm from the root tips, the xylem, primary phloem, endodermis, and exodermis autofluoresced yellow (Figs. 1B–1E), whereas the cell walls in the rest of the cortex fluoresced only slightly yellow. At 50 mm from the root tips, the secondary xylem fluorescence was intensely yellow; phellem and primary phloem fluoresced yellow, but not an "intense yellow" as seen in the root tips (Figs. 1F, 1G), and the two-year-old roots retained their cortex. In the three-year-old roots, the cortex was sloughed off; the secondary xylem and primary phloem fluoresced intensely yellow, while the phellem fluoresced brown (Fig. 1H), and the secondary phloem was dark. There were berberine deposits in the primary xylem, and larger deposits in the secondary xylem, phloem fibers, and phellem appearing gradually from the root apex to the base.

3.2 Structures of the Adventitious Roots

At 10 mm from the tips of the 80–150 mm-long adventitious roots, we observed an epidermis with hairs, a slightly lignified exodermis with Casparian bands and suberin lamellae (Figs. 2A–2C), and two primary xylem poles with only a few suberized endodermal walls. At 20 mm from the root tips, the endodermis was slightly lignified and had visible Casparian bands and suberin lamellae. The exodermis remained only slightly lignified (Figs. 2D–2F), and the epidermis had been sloughed off. At 30 mm from the tips, the secondary xylem and the endodermis and exodermis had intense Casparian bands under UV light that were suberized and lightly lignified (Figs. 2G–2I). We observed only a few passage cells in the endodermis. At 40 mm from the root tips, the secondary xylem had a cylindrical configuration and an endodermis that was lightly lignified (Figs. 3A–3C). The exodermis also had more lignin than at 30 mm. At 50 mm from the tips, dot-like lignified Casparian bands were observed in the phellem (Figs. 3D–3F), and the suberin lamellae of the phellem fluoresced brown under UV light (Figs. 1H, 3D, 3F). The cortex and exodermis were becoming sloughed off in this region. Deposits of berberine in the xylem walls appeared yellow under brightfield microscopy (Figs. 2I, 3C). The exodermis developed earlier than the endodermis at the root apex, and all roots had heavier suberin and less lignin in the endodermis and exodermis before the cortex sloughed off. The phellem had Casparian bands as well as suberin and lignin in the secondary structure of the roots.

3.3 Berberine Deposits in the Rhizomes

The rhizomes were composed of a cuticle, phellem, cortex, primary phloem, secondary phloem, secondary xylem, and pith (Figs. 4A, 4B). At the young rhizome internodes, the cuticle, secondary xylem, and primary phloem fluoresced yellow under UV light in the absence of staining (Figs. 4A–4C), and the cell walls in the cortex fluoresced light yellow. In the mature rhizomes, the cylindrical secondary xylem, adventitious roots in the cortex, and pith fluoresced yellow (Figs. 4D–4F), but fluorescence in the phellem was weak. In the petioles, the vascular bundles and sclerenchyma rings fluoresced yellow

(Figs. 4G, 4H). Berberine was deposited in the xylem, primary phloem walls, roots that had originated from the rhizomes, and the vascular bundles and sclerenchyma rings in the petioles. The mature rhizomes had ring-like secondary xylem, adventitious roots in the cortex, and phellem under the cuticle, whereas young rhizomes had dot-like secondary xylem. The rhizome structures were composed of a cuticle, cortex, a vascular cylinder with pith, a phellem, and secondary xylem in secondary growth.

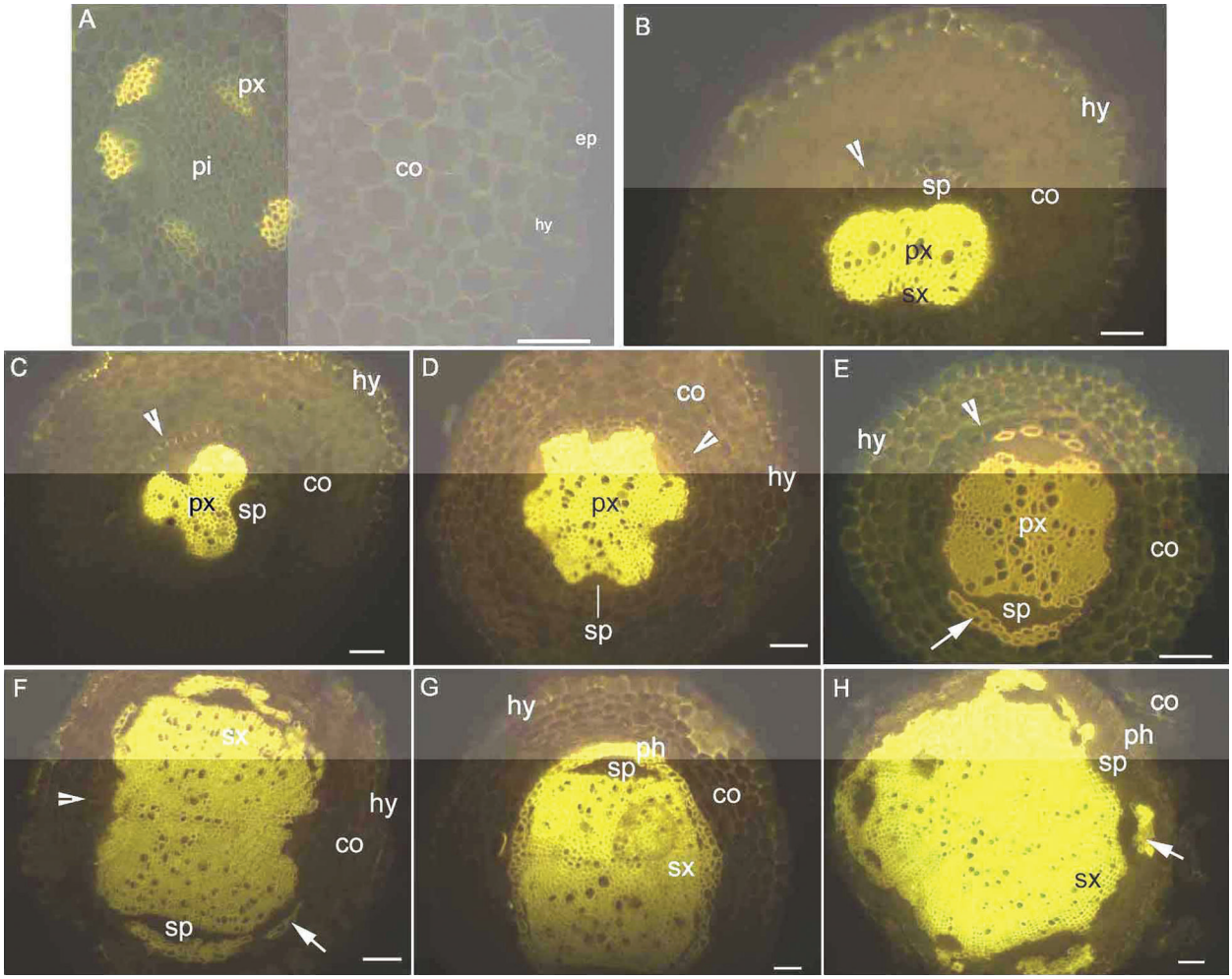

Figure 1: Photomicrographs of blue excitation (autofluorescence) of transverse sections of *Coptis chinensis* Franch. (Huanglian) adventitious roots. (A) 10 mm from the apex. (B–E) 30 mm from the apex. (F–G) 50 mm from the apex. (H) 50 mm from the apex of the base of the root of a three-year-old plant. Scale bars = 50 μm. Arrowheads indicate the endodermis; arrows indicate the primary phloem. Abbreviations: co, cortex; ep, epidermis; hy, hypodermis; ph, phellem; pi, pith; px, primary xylem; sp, secondary phloem; sx, secondary xylem

3.4 Structures of the Leaves

Between the central pith and cortex, the petioles exhibited a sclerenchyma ring with scattered vascular bundles (Figs. 4G, 4H, 5A, 5B), and the epidermis had a cuticle. Tab. 1 shows the morpho-anatomical characteristics of the blades: leaf area, tissue thicknesses, tissue densities, and epidermal features indicate few differences between sunny and shady leaves. The mesophyll was thicker, and the length of the

abaxial epidermis was longer for the sunny blades than the shady blades (Tab. 1). The main veins of the blades had vascular bundles surrounded by sclerenchyma rings (Figs. 5C, 5D). The leaf blades from both sunny and shady environments had an epidermis with a thin cuticle, stomata, and isolateral mesophyll tissue (Figs. 5C–5G; Tab. 1). The adaxial epidermis veins were puberulous (Figs. 5C, 5D, 5H). The sunny leaves also had sunburn spots (Fig. 5I). The leaves of Huanglian were composed of pith, sclerenchyma rings with vascular bundles, a cortex, an isolateral mesophyll, and a thin cuticle.

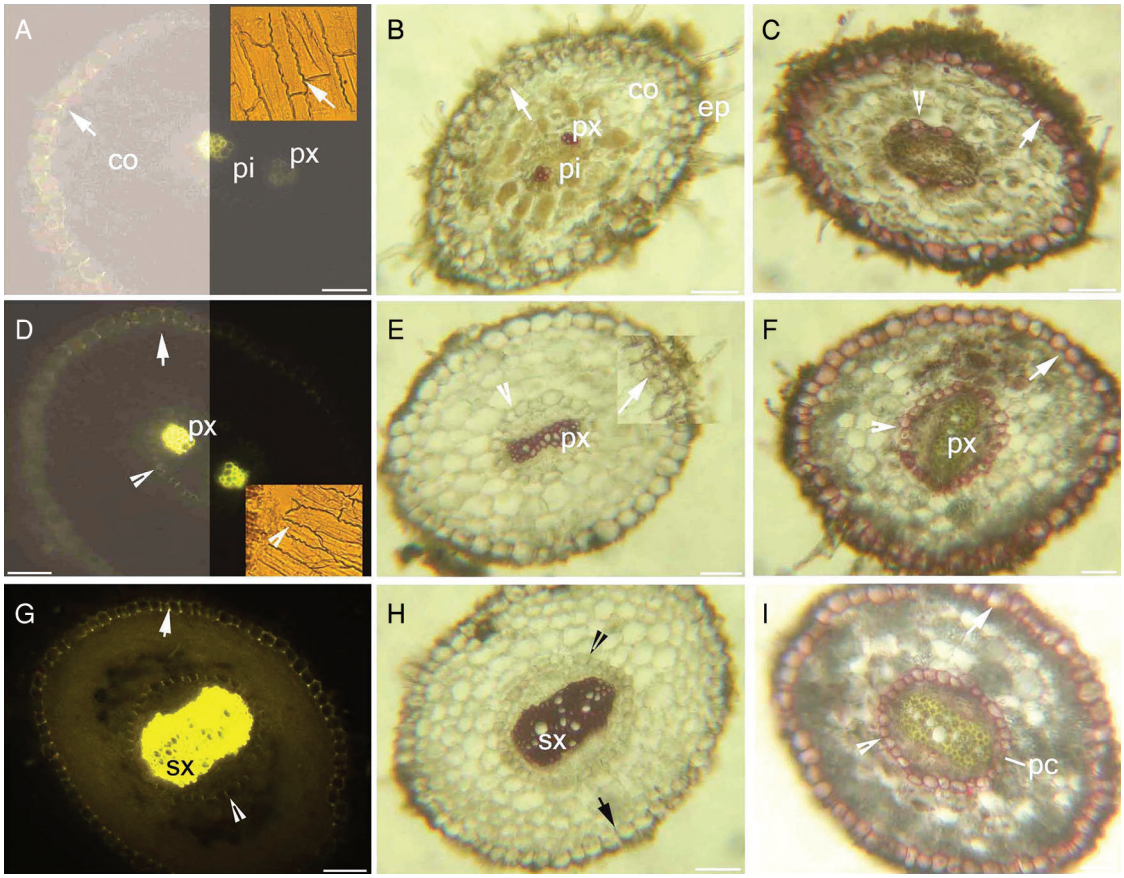

Figure 2: Photomicrographs of transverse sections of Huanglian adventitious roots from 10 to 30 mm. (A) 10 mm from the apex; BAB; the inset shows a Casparian band (arrows) on the exodermis after acid digestion. (B) 10 mm from the apex; Pg. (C) 10 mm from the apex; SR 7B. (D) 20 mm from the apex; BAB; the inset shows a Casparian band (arrowheads) on the endodermis following acid digestion. (E) 20 mm from the apex, the inset shows magnified exodermis, Pg. (F) 20 mm from the apex, SR 7B. (G) 30 mm from the apex, BAB. (H) 30 mm from the apex; Pg. (I) 30 mm from the apex, SR 7B. Scale bars = 50 μm. The arrowheads indicate the endodermis, and the arrows indicate the exodermis. Abbreviations: BAB, stained with berberine hemisulfate–aniline blue; co, cortex; ep, epidermis; pc, passage cell; Pg, stained with phloroglucinol–HCl; pi, pith; px, primary xylem; SR 7B, stained with Sudan red 7B; sx, secondary xylem

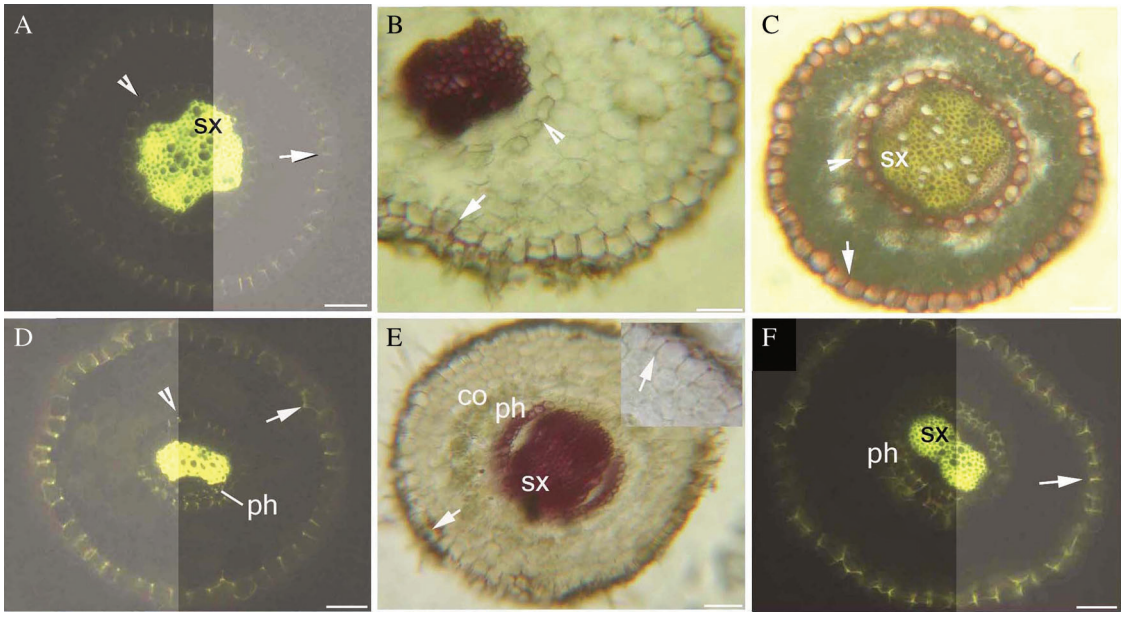

Figure 3: Photomicrographs of transverse sections of Huanglian adventitious roots from 40 to 50 mm. (A) 40 mm from the apex, BAB. (B) 40 mm from the apex, Pg. (C) 40 mm from the apex, SR 7B. (D) 50 mm from the apex, BAB. (E) 50 mm from the apex; the inset shows magnified exodermis, Pg. (F) 50 mm from the apex, BAB. The arrowheads indicate the endodermis, and the arrows indicate the exodermis. Scale bars = 50 μm. Abbreviations: BAB, stained with berberine hemisulfate–aniline blue; co, cortex; Pg, stained with phloroglucinol–HCl; ph, phellem; SR 7B, stained with Sudan red 7B; sx, secondary xylem

4 Discussion

The primary structures of Huanglian adventitious roots are known to have various archetypes in the cylinder, endodermis, cortex, exodermis, and epidermis [6,21] as well as a secondary structure of xylem, phloem and phellem. Interestingly, we observed that the cortex in Huanglian was retained and not sloughed off following secondary structure development, in contrast to the pattern observed in the land plant *Camellia sinensis* (L.) Kuntze [29]. The endodermis and exodermis had Casparian bands, suberin lamellae, and less lignin. The exodermis in *C. sinensis* first develops close to the root tips; Huanglian is intermediate between *C. sinensis* and wetland plants [16,18,19,25,29,30]. The roots had one layer of exodermis, similar to *Hydrocotyle sibthorpioides* Lam [30]., whereas *Typha* spp., *Iris germanica* L., *Cynodon dactylon* (L.) Pers., and *Zizania latifolia* (Griseb.) Turcz. ex Stapf have been reported to have two or more lignified layers [16,20,24,25]. The phellem in the roots of Huanglian had Casparian bands and suberin lamellae and was lignified, as observed in the stem periderm of *Pelargonium hortorum* L. H. Bailey and in the aged roots of *Camellia sinensis* (L.) Kuntze and *Alternanthera philoxeroides* (Mart.) Griseb [17,28,29]. The endodermis, exodermis, and phellem act as barriers, blocking water and ions from penetrating the tissue while allowing passage to individual cells [15–20,25].

The presence of berberine deposits in the xylem walls was confirmed by the yellow autofluorescence under epifluorescence microscopy. Additionally, studies have determined that berberine in the lignified xylem walls fluoresces yellow when stained exogenously [16–17,20,23–25]. The berberine deposits were directly observed under brightfield microscopy of the roots and rhizomes and in the sclerenchyma rings of the petioles [31,32]. In the present study, the berberine deposited in the xylem of Huanglian roots and

rhizomes and in the sclerenchyma rings of the petioles showed deposition patterns similar to those reported in *Mahonia* spp. and *Berberis* spp. [31–33].

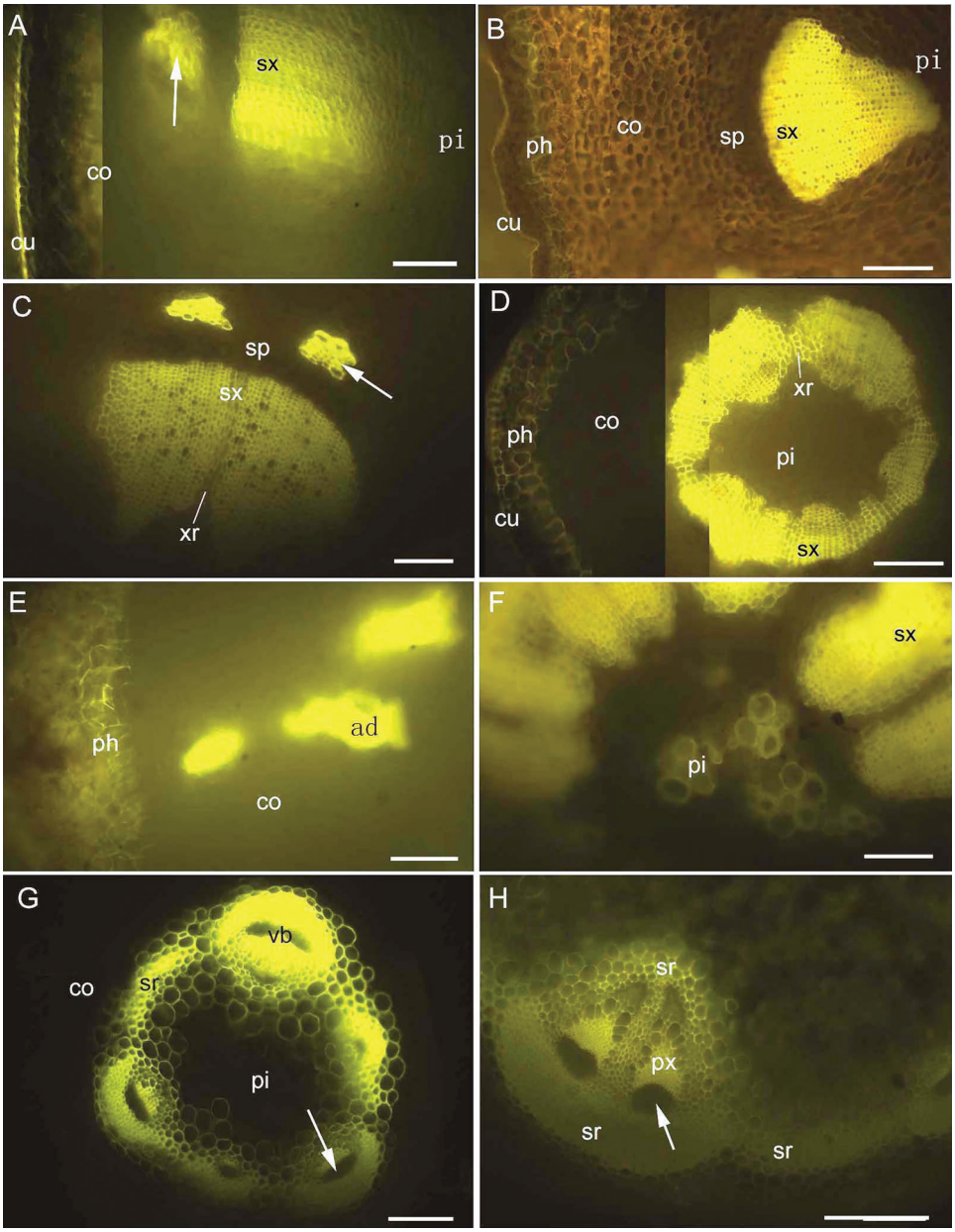

Figure 4: Photomicrographs of blue excitation (autofluorescence) of transverse sections of Huanglian rhizomes and petioles. (A) The young internode of a one-year-old rhizome; (B) the aged internode of a one-year-old rhizome; (C) the aged internode of a multi-year-old rhizome; (D) the aged internode of a multi-year-old rhizome; (E) the aged internode of a multi-year-old rhizome; (F) the aged internode of a multi-year-old rhizome; (G–H) at the base of the petiole. Scale bars = 100 μm. Arrows indicate the primary phloem. Abbreviations: ad, adventitious roots; co, cortex; cu, cuticle; ph, phellem; pi, pith; px, primary xylem; sp, secondary phloem; sr, sclerenchyma ring; sx, secondary xylem; vb, vascular bundles; xr, xylem rays

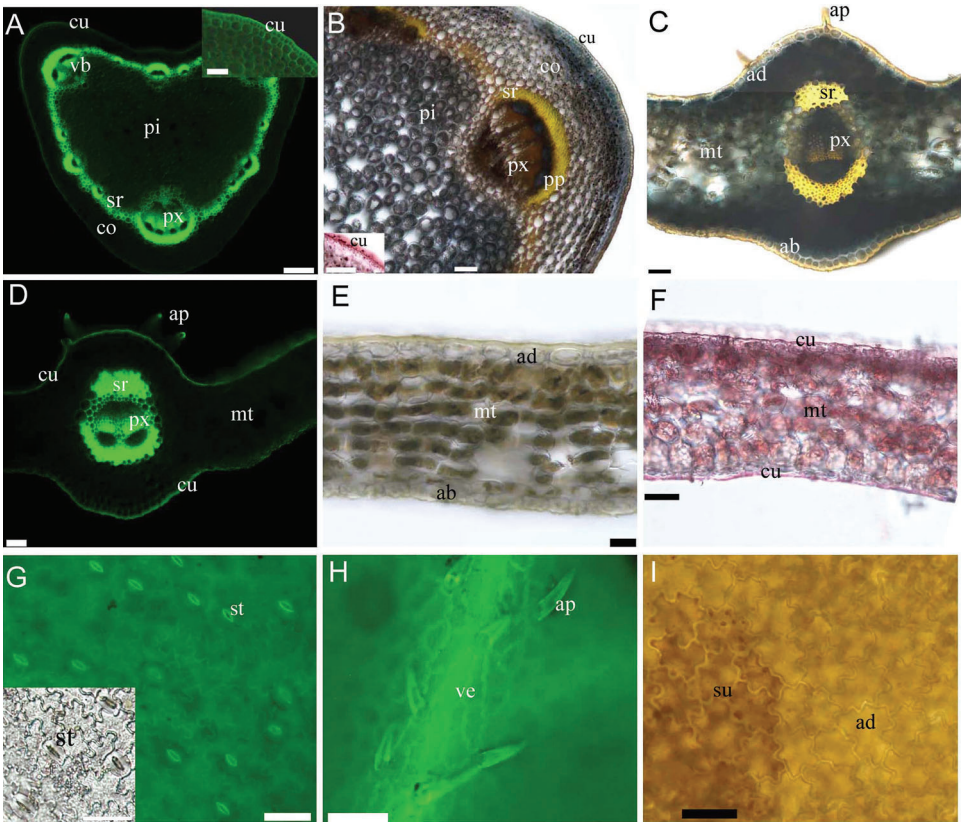

Figure 5: Photomicrographs of the (A–B) petioles, (C–H) shady leaves, and (I) sunny leaves. Panels C–F show the leaf blade adaxial side up. (A) Base petiole; BAB. (B) Base petiole; BAB under bright field; inset; SR 7B. (C) Main vein; BAB under bright field. (D) Main vein; BAB. (E) Blades; unstained. (F) Blades; SR 7B. (G) Blade surface; BAB; inset; unstained. (H) Blade adaxial surface; BAB. (I) Blade surface; unstained. Scale bars = 50 µm, except A = 200 µm. Abbreviations: ad, adaxial epidermis; ab, abaxial epidermis; ap, adaxially puberulous; co, cortex; cu, cuticle; mt, isolateral mesophyll tissue; pi, pith; pp, primary phloem; px, primary xylem; sr, sclerenchyma ring; st, stomata; su, sunburn spots; ve, vein; vb, vascular bundles

Exogenous berberine, an organic cation, has been used to stain lignified cell walls [16,17,23–25], and its utility as a tracer for assessing cell wall permeability has been investigated [16–20]. These results indicated that the exogenous berberine combined with the lignin in the cell walls and with potassium thiocyanate solution to form crystals [16–20,23–25]. However, Lu et al. [22] treated tissue sections with potassium mercuric iodide and discovered that berberine is deposited in crystal form in the parenchymal tissue of Huanglian. We observed that berberine is deposited in xylem and to a lesser extent in the parenchyma of the cortex. This differs from previous reports that berberine deposits were mainly localized to the parenchyma of the rhizome [22]. Here, we speculated that berberine is in an ionic state in the parenchyma tissue of Huanglian before it is transferred and deposited in the xylem [22,23,31–33]. Tocci et al. [34] reported xanthone biosynthesis in the exodermis and endodermis of *Hypericum perforatum* L. roots. We hypothesize that berberine is also synthesized in the parenchyma and stored in the xylem of Huanglian [22,23,25,34].

Flavonoids can enhance plant tolerance to cadmium (Cd), and they have a significant stimulatory effect on the symplastic transport of Cd in the roots of *Avicennia marina* (Forssk.) Vierh [35]. We speculated that berberine and flavonoids may have different ionic forms and thus different ion absorption functions

[22,23,25,35]. Berberine deposits in the xylem walls of Huanglian may occupy the space and interfere with absorption and transport of water and ions [15,18,19,23]. We propose that berberine deposition in the xylem and developing exodermis in the vicinity of the root tips may adversely affect the transport and absorption of water and ions, resulting in slow growth [15,18,19,23,35].

Table 1: Morphological and anatomical traits of blades and environmental data

Morphological traits	Sunny (Mean ± SE)	Shady (Mean ± SE)
Leaf area		
Length (cm)	9.56 ± 0.22	10.12 ± 0.63
Width (cm)	10.78 ± 0.34	11.60 ± 1.04
Thickness (μm)	220.40 ± 19.79	181.70 ± 6.06
Tissue thickness		
Adaxial cuticle (μm)	1.39 ± 0.10	1.40 ± 0.07
Abaxial cuticle (μm)	0.62 ± 0.05	0.59 ± 0.04
Mesophyll (μm)	142.16 ± 3.03	121.60 ± 4.65**
Adaxial epidermis (μm)	16.15 ± 0.85	16.38 ± 0.96
Abaxial epidermis (μm)	12.92 ± 0.71	11.78 ± 0.38
Tissue density		
Adaxial epidermis (n mm^2)	595.00 ± 12.60	616.80 ± 23.88
Abaxial epidermis (n mm^2)	576.80 ± 6.01	581.40 ± 9.59
Adaxial stomata (n mm^2)	286.60 ± 7.50	271.80 ± 3.57
Abaxial stomata (n mm^2)	278.20 ± 2.96	274.00 ± 5.16
Epidermal features		
Adaxial epidermis length (μm)	57.80 ± 1.93	56.60 ± 2.16
Adaxial epidermis width (μm)	47.04 ± 1.52	54.20 ± 3.06
Abaxial epidermis length (μm)	56.20 ± 1.46	50.40 ± 1.81*
Abaxial epidermis width (μm)	53.40 ± 3.14	51.40 ± 2.91
Adaxial stomatal length (μm)	26.50 ± 0.59	26.40 ± 0.51
Adaxial stomatal width (μm)	18.60 ± 0.51	17.60 ± 0.51
Abaxial stomatal length (μm)	27.00 ± 0.45	26.40 ± 0.51
Abaxial stomatal width (μm)	18.40 ± 0.51	17.40 ± 0.51

Note: * indicates a significant difference according to the *t*-test ($P < 0.05$), ** indicates a significant difference according to the *t*-test ($P < 0.01$).

The blades of Huanglian had isolateral mesophyll, which was also identified in *Panax* spp., *Adiantum reniforme* var. *sinense* Y. X. Lin, *Doryopteris pentagona* Pic. Serm., *Lygodium japonicum* (Thunb.) Sw., *Pteris multifida* Poir., *Nephrolepis cordifolia* (L.) C. Presl, *Adiantum capillus-veneris* L., and *Pteris ensiformis* cv. *victoriae* Bak [6–8,11,14,36]. The blades of Huanglian had isolateral mesophyll and thin cuticles, similar to other sciophytes such as *Panax* spp., *Lygodium japonicum*, *Pteris multifida*, *Nephrolepis cordifolia*, *Adiantum capillus-veneris*, *Pteris ensiformis* cv. *victoriae*, and *Doryopteris pentagona* [6,7,11,14,36]. The sunny leaves had thicker mesophyll, but they had sunburn spots under strong light, and they also had thin cuticles, suggesting that this species was adapted to shady environments. This contrasts with sunny or xeromorphic plants, such as *Cheilanthes glauca* (Cav.) Mett. and *Doryopteris triphylla* (Lam.) Christ, which have thick cuticles [6–12,14,36]. We suggest that Huanglian has adapted to low-light shady environments, and that this adaptation inevitably led to low photosynthetic efficiency, resulting in slow growth [6,7,9].

5 Conclusions

Huanglian exhibited isolateral mesophyll, thin cuticles, and an absence of tissue differentiation, suggesting a tolerance for shady environments [6–8,11,14]. Our results revealed that the exodermis is developed early, and the deposition of berberine in the xylem is located closest to the root tips. The structures of the leaves and adventitious roots of Huanglian may have adapted to low light as well as low absorption of water and ions, thus resulting in low photosynthetic efficiency and slow growth, all of which are highly suitable for shady environments [6–10,15,18,19,23,35–37]. These structural and histochemical features likely contribute to the slow growth of Huanglian.

Funding Statement: This work was supported by the Major Program on Technology Innovation of Hubei Province (2019ACA162), the Hubei Province Key Laboratory of Conservation Biology for Shennongjia Golden Monkey Opening Fund (SNJGKL202002), and the Engineering Research Center of Ecology and Agriculture Use of Wetland, Ministry of Education opening fund, Yangtze University (KFT202004).

Conflicts of Interest: The authors declare that they have no conflicts of interest to report regarding the present study.

References

1. Wang, X. K., Yang, P. Q., Chen, X. M. (1964). Ubre alkaloideaus *Coptis chinensis* Franch. var. *shihchuensis* wang. (V). *Acta Pharmaceutica Sinica, 11,* 389–392.
2. Xiao, P. G. (1984). Research pharmacognosy of traditional Chinese medicine material named *Coptis chinensis*. *Chinese Traditional and Herbal Drugs, 15,* 30–34.
3. Zhang, L., Zhang, X. P. (2006). The present research situation of plants of *Coptis* salisb in China. *Journal of Anhui Normal University (Natural Science), 29,* 368–371. DOI 10.3969/j.issn.1001-2443.2006.04.016.
4. Kamath, S., Skeels, M., Pai, A. (2009). Significant difference in alkaloid content of *coptis chinensis* (Huanglian), from its related American species. *Chinese Medicine, 4,* 1–4. DOI 10.1186/1749-8546-4-17.
5. Zhao, N., Li, L. Y., Bai, Z. C. (2015). Research status and prospect of traditional Chinese medicine material named *coptis chinensis*. *Journal of Chongqing University of Technology (Natural Science), 29,* 53–58. DOI 10.3969/j.issn.1674-8425(z).2015.01.010.
6. Yuan, W. J., Zhang, W. R., Shang, F. D. (2007). Study on the anatomical structure of vegetative organs of *coptis chinensis* and its pertinence to sciophyte conditions. *Journal of Henan University (Natural Science), 37(2),* 184–186. DOI 10.15991/j.cnki.411100.2007.02.018.
7. Lee, O. R., Nguyen, N. Q., Lee, K. H., Kim, Y. C., Seo, J. (2016). Cytohistological study of the leaf structures of *panax ginseng* meyer and *panax quinquefolius* L. *Journal of Ginseng Research, 41,* 463–468. DOI 10.1016/j.jgr.2016.08.001.
8. Crang, R., Lyons-Sobaski, S., Wise, R. (2019). *Plant anatomy: A concept-based approach to the structure of seed plants*, 1st edition. Springer, Gewerbestrasse, Switzerland. DOI 10.1007/978-3-319-77315-5_4.
9. Boardman, N. K. (1977). Comparative photo synthesis of sun and shade plant. *Annual Review of Plant Physiology, 28,* 355–357. DOI 10.1146/annurev.pp.28.060177.002035.
10. Givnish, T. J. (1988). Adaptation to sun and shade: A whole plant perspective. *Australian Journal of Plant Physiology, 15,* 63–92. DOI 10.1071/pp9880063.
11. Zhang, Z. H., Wu, X. X. (2013). Study on the anatomy structure of five species of fern leaves and its adaptability to sciophyte environment. *Journal of Huazhong Normal University (Natural Sciences), 47(6),* 840–843. DOI 10.19603/j.cnki.1000-1190.2013.06.020.
12. Shah, S. N., Ahmad, M., Zafar, M., Ullaha, F., Zamana, W. et al. (2019). Leaf micromorphological adaptations of resurrection ferns in northern Pakistan. *Flora, 255(6),* 1–10. DOI 10.1016/j.flora.2019.03.018.
13. Baer, A., Wheeler, J. K., Pittermann, J. (2020). Limited hydraulic adjustments drive the acclimation response of *pteridium aquilinum* (L.) kuhn to variable light. *Annals of Botany, 125(4),* 691–700. DOI 10.1093/aob/mcaa006.

14. Wu, D., Li, L. B., Ma, X. B., Huang, G. Y., Yang, C. D. (2020). Morphological and anatomical adaptations to dry, shady environments in *adiantum reniforme* var. *sinense* (Pteridaceae). *PeerJ, 8,* e9937. DOI 10.7717/peerj.9937.
15. Enstone, D. E., Peterson, C. A., Ma, F. (2003). Root endodermis and exodermis: Structure, function, and responses to the environment. *Journal of Plant Growth and Regulation, 21,* 335–351. DOI 10.1007/s00344-003-0002-2.
16. Yang, C. D., Zhang, X., Li, J., Bao, M. Z., Ni, D. J. et al. (2014). Anatomy and histochemistry of roots and shoots in wild rice (*Zizania latifolia* griseb.). *Journal of Botany, 2014,* Article ID 181727. DOI 10.1155/2014/181727.
17. Yang, C. D., Yang, X. L., Zhang, X., Zhou, C. Y., Zhang, F. et al. (2019). Anatomical structures of alligator weed (*Alternanthera philoxeroides*) suggest it is well adapted to the aquatic–terrestrial transition zone. *Flora, 253,* 27–34. DOI 10.1016/j.flora.2019.02.013.
18. Zhang, X., Hu, L., Yang, C. D., Zhou, C., Yuan, L. et al. (2017). Structural features of *phalaris arundinacea* L. in the jianghan floodplain of the Yangtze river, China. *Flora, 229,* 100–106. DOI 10.1016/j.flora.2017.02.016.
19. Zhang, X., Yang, C. D., Seago Jr, J. L. (2018). Anatomical and histochemical traits of roots and stems of *artemisia lavandulaefolia* and *a. selengensis* (Asteraceae) in the jianghan floodplain, China. *Flora, 239,* 87–97. DOI 10.1016/j.flora.2017.11.009.
20. Meyer, C. J., Seago, Jr. J. L., Peterson, C. A. (2009). Environmental effects on the maturation of the endodermis and multiseriate exodermis of *iris germanica* roots. *Annals of Botany, 103(5),* 687–702. DOI 10.1093/aob/mcn255.
21. Yang, J. M., Tang, H. G. (1984). An anatomical study on the root and the root stock of *coptis chinensis* franch. *Wuhan Botanical Research, 2,* 227–232.
22. Lu, G. L., Hu, Z. H. (1994). Histochemistry of berberine of *Coptis chinensis* Franch. rhizome. *Acta Botanica Boreali-occidentalia Sinica, 14,* 164–168. DOI CNKI:SUN:DNYX.0.1994-03-001.
23. Brundrett, M. C., Enstone, D. E., Peterson, C. A. (1988). A berberine–aniline blue fluorescent staining procedure for suberin, lignin and callose in plant tissue. *Protoplasma, 146,* 133–142. DOI 10.1007/BF01405922.
24. Seago Jr, J. L., Peterson, C. A., Enstone, D. E., Scholey, C. A. (1999). Development of the endodermis and hypodermis of *typha glauca* godr. and *T. angustifolia* L. roots. *Canadian Journal of Botany, 77,* 122–134. DOI 10.1139/b98-173.
25. Yang, C. D., Zhang, X., Zhou, C. Y., Seago Jr, J. L. (2011). Root and stem anatomy and histochemistry of four grasses from the jianghan floodplain along the Yangtze river, China. *Flora, 206,* 653–661. DOI 10.1016/j.flora.2010.11.011.
26. Jensen, W. A. (1962). *Botanical histochemistry–principles and practice*. San Francisco, CA, USA: WH Freeman.
27. Brundrett, M. C., Kendrick, B., Peterson, C. A. (1991). Efficient lipid staining in plant material with Sudan red 7B or fluorol yellow 088 in polyethylene glycol–glycerol. *Biotechnic and Histochemistry, 66,* 111–116. DOI 10.3109/10520299109110562.
28. Meyer, C. J., Peterson, C. A. (2011). Casparian bands occur in the periderm of *Pelargonium hortorum* stem and root. *Annals of Botany, 107,* 591–598. DOI 10.1093/aob/mcq267.
29. Hu, L. J., Yang, C. D., Yuan, L. Y., Liu, Z. X., Deng, C. H. et al. (2016). Study on the anatomy and barrier structure spatial-temporal developmental characters of adventitious root of *Camellia sinensis* cv. *Lichuanhong. Hubei Agricultural Sciences, 55,* 3662–3665. DOI 10.14088/j.cnki.issn0439-8114.2016.14.030.
30. Yang, C. D., Li, S. F., Yao, L., Ai, X. R., Cai, X. D. et al. (2015). A study of anatomical structure and apoplastic barrier characters of *Hydrocotyle sibthorpioides*. *Acta Prataculturae Sinica, 24,* 139–145. DOI 10.11686/cyxb2014246.
31. Greathouse, G. A., Watkins, G. M. (1938). Berberine as a factor in the resistance of *mahonia trifoliolata* and *M. swaseya* to phymatotrichum root. *American Journal of Botany, 25,* 743–748. DOI 10.2307/2436601.
32. Yi, L., Liang, Z. T., Peng, Y., Guo, P., Wong, L. L. et al. (2015). Histochemical evaluation of alkaloids in rhizome of *coptis chinensis* using laser microdissection and liquid chromatography/mass spectrometry. *Drug Testing and Analysis, 7,* 519–530. DOI 10.1002/dta.1703.
33. Cromwell, B. T. (1933). Experiments on the origin and function of berberine in *Berberis darwinii*. *Biochemical Journal, 27,* 863. DOI 10.1042/bj0270860.

34. Tocci, N., Gaid, M., Kaftan, F., Belkheir, A. K., Belhadj, I. et al. (2018). Exodermis and endodermis are the sites of xanthone biosynthesis in *hypericum perforatum* roots. *New Phytologist, 217,* 1099–1112. DOI 10.1111/nph.14929.

35. Li, J., Lu, H., Liu, J., Hong, H., Yan, C. (2015). The influence of flavonoid amendment on the absorption of cadmium in *avicennia marina* roots. *Ecotoxicology and Environmental Safety, 120,* 1–6. DOI 10.1016/j.ecoenv.2015.05.004.

36. Dematteis, B., Solís, S. M., Yesilyurt, J. C., Meza Torres, E. I. (2019). Comparative anatomy in four cheilanthoid ferns. *Boletin de la Sociedad Argentina Botanica, 54,* 203–214. DOI 10.31055/1851.2372.v54.n2.24365.

37. Evert, R. F. (2006). *Esau's plant anatomy: Meristems, cells, and tissues of the plant body: Their structure, function, and development*, 3rd edition. Hoboken, New Jersey, USA: Wiley-Interscience. DOI 10.1002/0470047380.ch10.